

# ALTERNATING SCHWARZ METHODS FOR PDE BASED MESH GENERATION

RONALD D. HAYNES \* AND ALEXANDER J. M. HOWSE †

**Abstract.** To solve boundary value problems with moving fronts or sharp variations, moving mesh methods can be used to achieve reasonable solution resolution with a fixed, moderate number of mesh points. Such meshes are obtained by solving a nonlinear elliptic differential equation in the steady case, and a nonlinear parabolic equation in the time-dependent case. To reduce the potential overhead of adaptive PDE based mesh generation here we consider solving this problem by various alternating Schwarz domain decomposition methods. Convergence results are established for alternating iterations with classical and optimal transmission conditions on an arbitrary number of subdomains. An analysis of a colouring algorithm is given which allows the subdomains to be grouped for parallel computation. A first result is provided for the generation of time dependent meshes by an alternating Schwarz algorithm on an arbitrary number of subdomains. The paper concludes with numerical experiments illustrating the relative contraction rates of the iterations discussed.

**Key words.** Domain Decomposition, Schwarz Methods, Equidistribution, Moving Meshes

**AMS subject classifications.** 65M55, 65N55, 65L50, 65M50, 65N50

**1. Introduction.** The efficient solution of differential equations involving one or more spatial variables often requires *adaptive methods* to dynamically adjust the spatial mesh. Such adjustments can be achieved in a variety of ways. The *r-refinement* approach is a class of adaptive methods which move, or relocate, a fixed number of mesh points during the computation to best resolve the solution. Such PDE based mesh generation adds a sometimes burdensome overhead to the cost of solving the physical PDE. This motivates the study of algorithms capable of a divide and conquer approach, solving the mesh PDE in small pieces, possibly on multiple compute cores, and recombining the pieces to generate the global mesh. In this paper we consider the application of alternating Schwarz type domain decomposition methods to the PDE based mesh generation problem.

In one spatial dimension, a common way to distribute the mesh points is the *equidistribution principle*, first introduced by de Boor [3, 4]. A strictly positive function  $M(x)$  is a *mesh density function* [15] (or a *monitor function* [2, 12, 14]) for a differential equation if  $M(x)$  indicates the magnitude of error between the exact and numerical solutions at all points  $x$  in the (physical) domain. Mesh points will naturally cluster where  $M$  is large.

Given such a  $M(x)$  and some integer  $N > 1$ , equidistribution over a bounded interval  $[a, b]$  requires finding a mesh  $\{x_i\}_1^N$ , with  $x_1 = a$  and  $x_N = b$ , such that  $M(x)$  is evenly distributed over the  $N - 1$  subintervals. That is, we require

$$(1.1) \quad \int_a^{x_i} M(x) dx = \frac{(i-1)}{(N-1)} \int_a^b M(x) dx, \quad i = 1, \dots, N.$$

It has been shown in the continuous case (e.g. see [15]) that for a given integer  $N > 1$  there exists a unique mesh satisfying (1.1) for any strictly positive  $M(x)$ . In the discrete case, if  $M(x)$  has sufficient smoothness and  $N$  large enough, then the sequence of meshes obtained by *de Boor's* algorithm will converge to a discrete approximation of the equidistributing mesh [17].

In a continuous form, we seek a coordinate transformation

$$x = x(\xi), \quad \xi \in [0, 1], \quad x(0) = a, \quad x(1) = b,$$

---

\*Department of Mathematics and Statistics, Memorial University of Newfoundland, St. John's, Newfoundland. (rhaynes@mun.ca). Questions, comments, or corrections to this document may be directed to that email address.

†Department of Mathematics and Statistics, Memorial University of Newfoundland, St. John's, Newfoundland. (z37ajmh@mun.ca).

so that

$$\int_a^{x(\xi_i)} M(x) dx = \xi_i \int_a^b M(x) dx, \quad i = 1, \dots, N,$$

where

$$\xi_i = \frac{(i-1)}{(N-1)}, \quad i = 1, \dots, N,$$

is a uniform partition of the computational coordinate  $\xi \in [0, 1]$ . We say that  $x = x(\xi)$  is an *equidistributing coordinate transformation* [15] for  $M(x)$  if it satisfies

$$(1.2) \quad \int_a^{x(\xi)} M(x) dx = \xi \int_a^b M(x) dx \quad \forall \xi \in (0, 1).$$

Differentiating twice with respect to  $\xi$  and assuming sufficient smoothness, we obtain the nonlinear boundary value problem

$$(1.3) \quad \frac{d}{d\xi} \left( M(x) \frac{dx}{d\xi} \right) = 0, \quad x(0) = a, \quad x(1) = b,$$

for the required mesh transformation. We illustrate such a transformation in Figure 1.1, where we plot the function  $u(x) = \frac{1}{2}(1 - \tanh(20x - 10))$  over  $[0, 1]$  using an equidistributed mesh obtained by solving (1.3) using the arclength monitor function  $M(x) = \sqrt{1 + u_x^2}$ . The location of the computed mesh points are indicated by ticks below the  $x$ -axis.

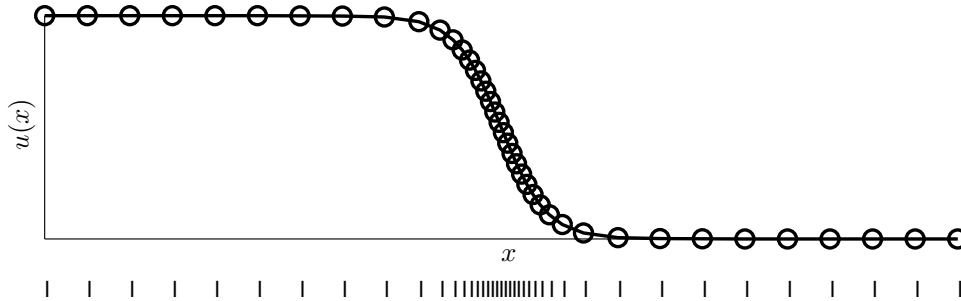


FIG. 1.1. A function with a sharp front plotted on an equidistributed mesh.

In general, (1.3) is coupled, through  $M(x)$ , to a PDE for the physical solution  $u(x)$ . However, we will consider the solution of (1.3) assuming  $u(x)$  is specified, which is not unrealistic in practice, as the mesh PDE and the physical solution are often solved in an alternating fashion.

We consider solving (1.3) via a domain decomposition (DD) approach. DD is used to express an often prohibitively large, computationally expensive problem as several smaller problems which can be solved, sometimes in parallel, in hopes of obtaining the solution to the original problem more efficiently. The text [16] by Toselli and Widlund serves as a comprehensive technical reference for many popular DD methods, and the article [6] by Gander provides a historical overview of the Schwarz DD methods used in this paper.

In the one dimensional case governed by (1.3), the typical DD approach is to decompose the interval  $[0, 1]$  into  $S$  sub-intervals  $[\alpha_i, \beta_i]$  which satisfy  $\alpha_1 = 0, \beta_S = 1$ , and

$$\alpha_i \leq \beta_{i-1} < \alpha_{i+1}, \quad i = 2, \dots, S-1.$$

This serves to ensure adjacent subdomains have a non-empty intersection and that non-adjacent subdomains are disjoint. An example is presented in Figure 1.2.

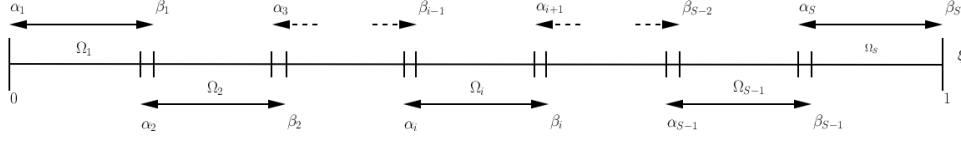


FIG. 1.2. The domain  $\Omega = [0, 1]$  decomposed into  $S$  subdomains.

Over each sub-interval we solve a sub-problem

$$\frac{d}{d\xi} \left( M(x_i) \frac{dx_i}{d\xi} \right) = 0, \quad \xi \in [\alpha_i, \beta_i],$$

subject to appropriately chosen transmission boundary conditions which communicate solution information between adjacent sub-problems. The goal is to eventually obtain the original mesh transformation  $x(\xi)$  in terms of the sub-interval solutions  $x_i(\xi)$  by solving these  $S$  smaller subdomain problems iteratively.

In [7] Gander and Haynes prove convergence results for three types of parallel DD methods to solve (1.3). The transmission conditions, in order of increasing efficiency, give rise to *classical Schwarz*, *optimized Schwarz* and *optimal Schwarz* methods. The classical Schwarz algorithm uses simple Dirichlet boundary conditions with the restriction that subdomains must overlap, the optimized Schwarz algorithm uses modified (nonlinear) Robin type boundary conditions, and the optimal Schwarz algorithm requires the use of nonlocal integral operators. As the complexity of information used in the transmission conditions increase there is a corresponding improvement in the rate of convergence of the DD iteration, with the optimal conditions theoretically achieving convergence in two iterations on two subdomains. The authors also introduce a parallel classical Schwarz algorithm to solve an implicit time discretized version of MMPDE5, a time-dependent relaxation of the equidistribution principle [15]:

$$(1.4) \quad \frac{\partial x}{\partial t} = \frac{1}{\tau} \frac{d}{d\xi} \left( M(x) \frac{dx}{d\xi} \right), \quad \xi \in [0, 1], \quad t \in [0, T].$$

The domain decomposition algorithms presented in [7] have been developed to allow the subdomain problems to be solved in parallel. Here we consider *alternating Schwarz* algorithms where the subdomain problems are solved sequentially, each subdomain using immediately updated transmission data to attain faster convergence. Such alternating methods for mesh generation have been briefly introduced in [8], where the convergence of an alternating classical Schwarz iteration has been established for two subdomains. Here we both extend the existing parallel classical Schwarz results for mesh generation on an arbitrary number of subdomains (from [7]) to the alternating case (Theorem 3.3) and generalize the optimal Schwarz analysis and the results for the generation of time dependent meshes to an arbitrary number of subdomains (Theorems 4.2 and 5.4). The later two theorems are not simply extensions of the existing results for the parallel iterations — no such optimal Schwarz results for the steady problem or classical Schwarz results for the time dependent problem on an arbitrary number of subdomains have appeared in the literature for this nonlinear boundary value problem. Moreover, in situations where we have adapted existing parallel Schwarz results to the alternating case, the details of the proofs are not simple notational modifications of the proofs of

the parallel Schwarz results. In addition, by using an approach similar to a red-black coloring for Gauss-Seidel [5], we show that the alternating iteration can be implemented in parallel while retaining the improved convergence characteristic of alternating methods; see Theorems 3.6 and 3.7. This is not the first use of such coloring methods for DD, cf. [1, 16] for linear problems.

The remainder of this paper is organized as follows. In Section 2 we collect several preliminary results, including well-posedness of the subdomain problems, which are required in the following analysis. In Section 3 we present two alternating classical Schwarz iterations for multiple subdomains. The first is the standard alternating approach, where each subdomain problem is solved sequentially, and the latter is a red-black coloring approach, which attempts to capture the best of both worlds, promising faster convergence without sacrificing the use of parallel computation. In Section 4 we provide results pertaining to alternating classical Schwarz iterations for the generation of time dependent meshes on an arbitrary number of subdomains. In Section 5 we present an overlapping optimal Schwarz method for steady mesh generation on an arbitrary number of subdomains. Section 6, for completeness, includes an alternating optimized Schwarz method for steady mesh generation which provide approximations of the optimal transmission conditions from the previous section. Section 7 presents numerical examples to illustrate the theoretical results, and finally Section 8 concludes with a summary and indicates future areas of study.

**2. Preliminaries.** Throughout this paper, we consider the solution of the differential equation (1.3) with a specified function  $M(x)$ , subject to various boundary conditions. We begin by noting the existence and uniqueness of a solution to this differential equation subject to Dirichlet boundary conditions, as stated in Lemma 2.1 of [7], which we reproduce here.

LEMMA 2.1. *Consider the following BVP on an arbitrary subdomain  $(\alpha, \beta) \subset \Omega = (0, 1)$ ,*

$$(2.1) \quad \frac{d}{d\xi} \left( M(x) \frac{dx}{d\xi} \right) = 0, \quad x(\alpha) = \gamma_\alpha, x(\beta) = \gamma_\beta.$$

*If  $M$  is differentiable and bounded away from zero and infinity, i.e. there exists  $\check{m}$  and  $\hat{m}$  such that  $0 < \check{m} \leq M(x) \leq \hat{m} < \infty$  for all  $x$ , then this BVP has a unique solution given implicitly by*

$$(2.2) \quad \int_{\gamma_\alpha}^{x(\xi)} M(\tilde{x}) d\tilde{x} = \frac{\xi - \alpha}{\beta - \alpha} \int_{\gamma_\alpha}^{\gamma_\beta} M(\tilde{x}) d\tilde{x}, \quad \xi \in (\alpha, \beta).$$

A simple consequence of this Lemma which will be used in several proofs is the following corollary.

COROLLARY 2.2. *For any  $\tilde{\xi} \in (0, 1)$ , the solution  $x(\xi)$  which solves (1.3) satisfies the equation*

$$\int_0^{x(\tilde{\xi})} M(\tilde{x}) d\tilde{x} = \tilde{\xi} \int_0^1 M(\tilde{x}) d\tilde{x}.$$

The following expressions, which also follow from Lemma 2.1, will be used in the proof of convergence for the optimal Schwarz iteration.

COROLLARY 2.3. *Suppose the domain  $[0, 1]$  is decomposed into subdomains  $[0, \beta]$  and  $[\alpha, 1]$ , with  $\alpha \leq \beta$ . Then the following hold:*

(i) The function  $x(\xi)$  solving

$$\frac{d}{d\xi} \left( M(x) \frac{dx}{d\xi} \right) = 0, \quad \xi \in [0, \beta]$$

with  $x(0) = 0$  and  $x(\beta)$  a known value satisfies

$$(2.3) \quad \int_0^{x(\xi)} M(\tilde{x}) d\tilde{x} = \frac{\xi}{\xi_u} \int_0^{x(\xi_u)} M(\tilde{x}) d\tilde{x} \quad \text{for } 0 \leq \xi \leq \xi_u,$$

where  $\xi_u \leq \beta$ .

(ii) The function  $x(\xi)$  solving

$$\frac{d}{d\xi} \left( M(x) \frac{dx}{d\xi} \right) = 0, \quad \xi \in [\alpha, 1]$$

with  $x(1) = 1$  and  $x(\alpha)$  a known value satisfies

$$(2.4) \quad \int_{x(\xi)}^1 M(\tilde{x}) d\tilde{x} = \frac{1-\xi}{1-\xi_l} \int_{x(\xi_l)}^1 M(\tilde{x}) d\tilde{x} \quad \text{for } \xi_l \leq \xi \leq 1,$$

where  $\xi_l \geq \alpha$ .

In Section 6 we will consider (1.3) subject to nonlinear Robin type conditions:

$$(2.5) \quad \frac{d}{d\xi} \left( M(x) \frac{dx}{d\xi} \right) = 0, \quad x(0) = 0, \quad M(x)x_\xi + px \Big|_\beta = \gamma_\beta,$$

and

$$(2.6) \quad \frac{d}{d\xi} \left( M(x) \frac{dx}{d\xi} \right) = 0, \quad M(x)x_\xi - px \Big|_\beta = \gamma_\beta, \quad x(1) = 1,$$

where  $p$  and  $\gamma_\beta$  are constants and  $\beta \in (0, 1)$  is fixed. Conditions under which these equations have unique solutions were stated in Lemmas 2.2 and 2.3 of [7], we reproduce them here as Lemmas 2.4 and 2.5.

LEMMA 2.4. *Under the assumptions of Lemma 2.1 the BVP (2.5) has a unique solution for all  $p > 0$  given implicitly by*

$$(2.7) \quad \int_0^{x(\xi)} M(\tilde{x}) d\tilde{x} = (\gamma_\beta - px(\beta))\xi, \quad \text{for } \xi \in (0, \beta).$$

LEMMA 2.5. *Under the assumptions of Lemma 2.1 the BVP (2.6) has a unique solution for all  $p > 0$  given implicitly as*

$$(2.8) \quad \int_{x(\xi)}^1 M(\tilde{x}) d\tilde{x} = (\gamma_\beta + px(\beta))(1 - \xi), \quad \text{for } \xi \in (\beta, 1).$$

In what follows  $\|\cdot\|_\infty$  denotes the usual  $L^\infty$  norm.

**3. Alternating Classical Schwarz Algorithms for Steady Mesh Generation.** In this section, we prove convergence of the alternating classical Schwarz algorithm for steady mesh generation on an arbitrary number of subdomains. We also present an alternating iteration which has been parallelized, by a method similar to that of the red-black coloring for Gauss-Seidel, to take advantage of parallel computation without sacrificing the improved convergence of alternating methods.

**3.1. Arbitrary Number of Subdomains.** We decompose  $\Omega = [0, 1]$  into  $S \geq 2$  subdomains  $\Omega_i = [\alpha_i, \beta_i]$  for  $i = 1, \dots, S$ , where  $\alpha_{i+1} < \beta_i$  for  $i = 1, \dots, S-1$  and  $\beta_i < \alpha_{i+2}$  for  $i = 1, \dots, S-2$ ; see Figure 1.2. The special case of two subdomains was considered in [8]. Consult [13] to see the details of how the result generalizes for the special cases of  $S = 3$  and  $S = 4$  subdomains. Here we will consider the general case and will assume that  $S > 3$  in what follows.

We denote by  $x_i(\xi)$  the solution over  $\Omega_i$  which is equal to the single domain solution throughout  $\Omega_i$  and satisfies

$$(3.1) \quad (M(x_i)x_{i,\xi})_\xi = 0, \quad x_i(\alpha_i) = x_{i-1}(\alpha_i), \quad x_i(\beta_i) = x_{i+1}(\beta_i), \quad i = 1, \dots, S,$$

where  $\alpha_1 = 0$ ,  $\beta_S = 1$ , and we define  $x_0(\alpha_1) = 0$  and  $x_{S+1}(\alpha_S) = 1$ . The alternating Schwarz DD iteration is given by

$$(3.2) \quad (M(x_i^n)x_{i,\xi}^n)_\xi = 0, \quad x_i^n(\alpha_i) = x_{i-1}^n(\alpha_i), \quad x_i^n(\beta_i) = x_{i+1}^{n-1}(\beta_i), \quad i = 1, \dots, S,$$

where we have defined  $x_0^n(\alpha_1) \equiv 0$  and  $x_{S+1}^n(\alpha_S) \equiv 1$ .

Define the error on the  $i$ th subdomain, at iteration  $n$ , as

$$(3.3) \quad e_i^n(\xi) = \int_{x_i(\xi)}^{x_i^n(\xi)} M(\tilde{x}) d\tilde{x},$$

for  $i = 1, \dots, S$ . Convergence is demonstrated by showing this error measure contracts to zero on all subdomains. As  $M$  is bounded away from zero,

$$\lim_{n \rightarrow \infty} e_i^n(\xi) = 0 \quad \text{implies} \quad \lim_{n \rightarrow \infty} |x_i(\xi) - x_i^n(\xi)| = 0.$$

We can compute this measure of the error on each subdomain explicitly. Introducing the values  $e_0^n(\alpha_1) \equiv 0$  and  $e_{S+1}^n(\alpha_S) \equiv 0$  for notational convenience we have the following result.

LEMMA 3.1. *The error on each subdomain satisfies*

$$(3.4) \quad e_i^n(\xi) = \frac{1}{\beta_i - \alpha_i} [(\xi - \alpha_i)e_{i+1}^{n-1}(\beta_i) + (\beta_i - \xi)e_{i-1}^n(\alpha_i)], \quad \xi \in [\alpha_i, \beta_i],$$

for  $i = 1, \dots, S$ .

*Proof.* Subtract (3.1) from (3.2) and differentiate the error expression (3.3) twice. Comparing these two results, we find that the error satisfies the simple linear BVP

$$\frac{d^2 e_i^n}{d\xi^2} = 0, \quad e_i^n(\alpha_i) = e_{i-1}^n(\alpha_i), \quad e_i^n(\beta_i) = e_{i+1}^{n-1}(\beta_i),$$

for  $i = 1, \dots, S$ . The result follows from direct integration and applying the given boundary conditions.  $\square$

Following [9], we introduce the quantities:

$$(3.5) \quad r_i = \frac{\beta_{i-1} - \alpha_i}{\beta_i - \alpha_i}, \quad p_i = \frac{\beta_i - \beta_{i-1}}{\beta_i - \alpha_i}, \quad q_i = \frac{\alpha_{i+1} - \alpha_i}{\beta_i - \alpha_i}, \quad \text{and} \quad s_i = \frac{\beta_i - \alpha_{i+1}}{\beta_i - \alpha_i}.$$

If the quantities  $r_i, s_i, p_i, q_i$  are constants then it is useful to introduce the quantities  $r, s, p$  and  $q$ ; we note  $r = s$  and  $p = q$  and  $p = 1 - r$ .

By using the quantities (3.5) in (3.4) and applying the triangle inequality we obtain the bounds on the error in Lemma 3.2.



where the contraction rate is bounded by:

$$\rho(M_e) \leq 1 - (1-r)r^{S-2},$$

where  $r$  is the common overlap ratio.

*Proof.* We show that  $\rho(M_e) < 1$ . The assumptions on the choice of the subdomains ensure the quantities (3.5) are non-negative, hence the matrix  $M_e$  is non-negative. The row sum

$$(p_S s_{S-1} \cdots s_2 q_1) + \cdots + p_S s_{S-1} q_{S-2} + p_S q_{S-1}$$

can be expressed using nested products as

$$p_S (s_{S-1} (s_{S-2} (\cdots (s_2 q_1 + q_2) \cdots) + q_{S-2}) + q_{S-1}).$$

We know that each  $q_i < 1$  and that  $q_i + s_i = 1$ . Starting at the innermost term, we have  $s_2 q_1 + q_2 < s_2 + q_2 = 1$ . Moving to the next set of brackets, we have  $s_3 (s_2 q_1 + q_2) + q_3 < s_3 + q_3 = 1$ . Proceeding in this manner, we know that each term contained within brackets will be less than one in magnitude, and as such we have

$$p_S (s_{S-1} (s_{S-2} (\cdots (s_2 q_1 + q_2) \cdots) + q_{S-2}) + q_{S-1}) < p_S < 1.$$

Similarly, as  $p_i + r_i = 1$ , the row sum is bounded as

$$(p_{S-1} s_{S-2} \cdots s_2 q_1) + \cdots + p_{S-1} s_{S-2} q_{S-3} + p_{S-1} q_{S-2} + r_{S-1} < p_{S-1} + r_{S-1} = 1.$$

We see this holds if we consider any row of the matrix, hence we must have  $\|M_e\|_\infty < 1$  and the iteration converges.

If we make the simplifying assumption that all subdomains are of equal size and we have a common overlap ratio  $r$  then we have the matrix

$$M_e = \begin{bmatrix} p^2 & r & & & & & \\ p^2 r & p^2 & r & & & & \\ p^2 r^2 & p^2 r & p^2 & r & & & \\ \vdots & \vdots & \vdots & \ddots & \ddots & & \\ & & & & p^2 & r & \\ p^2 r^{S-2} & \dots & & & p^2 r & p^2 & \end{bmatrix}.$$

From simple calculations, we find

$$\|M_e\|_\infty = p^2(1 + \cdots + r^{S-3}) + r = 1 - (1-r)r^{S-2},$$

which is an upper bound on the contraction rate.

We know  $|x_i^{n+1}(\xi) - x(\xi)| \leq \frac{1}{\tilde{m}} |e_i^{n+1}(\xi)|$ . Furthermore,  $|e_i^{n+1}(\xi)|$  is bounded by the maximum of its boundary values, thus:

$$\begin{aligned} |x_i^{n+1}(\xi) - x(\xi)| &\leq \frac{1}{\tilde{m}} |e_i^{n+1}(\xi)| \leq \frac{1}{\tilde{m}} \max \{|e_{i+1}^n(\beta_i)|, |e_{i-1}^n(\alpha_i)|\} \\ &\leq \frac{1}{\tilde{m}} \max \{|e_{i+1}^n(\beta_i)|, |e_{i-1}^n(\alpha_i)|\} \leq \frac{1}{\tilde{m}} \|e^n\|_\infty \\ &\leq \frac{1}{\tilde{m}} \|e^n\|_2 \leq \frac{1}{\tilde{m}} (\rho(M_e))^n \|e^0\|_2. \end{aligned}$$

Taking the supremum gives the  $L^\infty$  bound in the theorem statement.  $\square$



**3.2. A Red-Black Alternating Classical Schwarz Method.** The previous multidomain iteration is similar to the Gauss-Seidel iterative technique for solving linear systems, determining an improved approximation to each component of the solution sequentially. Gauss-Seidel can be implemented in parallel by partitioning the elements of the solution vector into different sets, solving for all members of a set simultaneously, and using these values when solving for the next set of elements. For instance, if we alternately color each component either red or black, we solve for all of the similarly colored components in parallel [5]. Similarly, if we appropriately partition the subdomains into two sets, we are able to solve all subdomain problems from each set in parallel while still maintaining the improved convergence which is characteristic of alternating methods. As in the previous case, we decompose the domain  $\Omega = [0, 1]$  into  $S > 2$  overlapping subdomains  $\Omega_i = [\alpha_i, \beta_i]$  for  $i = 1, \dots, S$ , where  $\alpha_{i+1} < \beta_i$  for  $i = 1, \dots, S-1$  and  $\beta_i < \alpha_{i+2}$  for  $i = 1, \dots, S-2$ . We denote by  $x_i(\xi)$  the original, single domain solution restricted to  $\Omega_i$ .

We now consider the the following classical Schwarz iteration. For  $i = 1, \dots, S$ : if  $i$  is odd, then

$$(3.10) \quad (M(x_i^n x_{i,\xi}^n))_\xi = 0, \quad x_i^n(\alpha_i) = x_{i-1}^{n-1}(\alpha_i), \quad x_i^n(\beta_i) = x_{i+1}^{n-1}(\beta_i),$$

and if  $i$  is even, then

$$(3.11) \quad (M(x_i^n x_{i,\xi}^n))_\xi = 0, \quad x_i^n(\alpha_i) = x_{i-1}^n(\alpha_i), \quad x_i^n(\beta_i) = x_{i+1}^n(\beta_i),$$

where we have defined  $x_0^n(\alpha_1) \equiv 0$  and  $x_{S+1}^n(\beta_S) \equiv 1$ . If  $S$  is even, then for each DD iteration we solve two sets of  $S/2$  boundary value problems, using the results from the odd subdomains to provide updated boundary conditions for the even subdomains. If  $S$  is odd, we first solve the  $(S+1)/2$  odd subdomain problems, then the  $(S-1)/2$  even subdomain problems. In either case, we solve all odd numbered subdomain problems in parallel, then all even numbered subdomain problems in parallel.

We define the error on the  $i$ th subdomain at iteration  $n$  using (3.3), for  $i = 1, \dots, S$ , and show convergence by proving this measure contracts to zero on all subdomains. The error on each subdomain is given explicitly in the following Lemma. We again define  $e_0^n(\alpha_1) \equiv 0$  and  $e_{S+1}^n(\beta_S) \equiv 0$ .

LEMMA 3.4. *The error on subdomain  $\Omega_i = [\alpha_i, \beta_i]$ ,  $i = 1, \dots, S$ , satisfies*

$$(3.12) \quad e_i^n(\xi) = \begin{cases} \frac{1}{\beta_i - \alpha_i} [(\xi - \alpha_i)e_{i+1}^{n-1}(\beta_i) + (\beta_i - \xi)e_{i-1}^{n-1}(\alpha_i)], & \text{if } i \text{ is odd,} \\ \frac{1}{\beta_i - \alpha_i} [(\xi - \alpha_i)e_{i+1}^n(\beta_i) + (\beta_i - \xi)e_{i-1}^n(\alpha_i)], & \text{if } i \text{ is even.} \end{cases}$$

The proof of Lemma 3.4 is nearly identical to Lemma 3.1 and hence is omitted. We use (3.12) to relate the error on subdomain  $i$  at iteration  $n$  to the error on subdomain  $i$  and its neighbors at iteration  $n-1$ . By using the quantities defined in (3.5) we find the recursive relationships stated in Lemma 3.5.

LEMMA 3.5. *The error at the interface  $\xi = \beta_{i-1}$ ,  $i = 2, \dots, N$  satisfies*

$$(3.13) \quad |e_i^{n+1}(\beta_{i-1})| \leq r_i r_{i+1} |e_{i+2}^n(\beta_{i+1})| + r_i p_{i+1} |e_i^n(\alpha_{i+1})| + p_i q_{i-1} |e_i^n(\beta_{i-1})| + p_i s_{i-1} |e_{i-2}^n(\alpha_{i-1})|,$$

while at  $\xi = \alpha_{i+1}$ ,  $i = 1, \dots, N-1$  we have

$$(3.14) \quad |e_i^{n+1}(\alpha_{i+1})| \leq q_i r_{i+1} |e_{i+2}^n(\beta_{i+1})| + q_i p_{i+1} |e_i^n(\alpha_{i+1})| + s_i q_{i-1} |e_i^n(\beta_{i-1})| + s_i s_{i-1} |e_{i-2}^n(\alpha_{i-1})|.$$

*Proof.* Inequality (3.13) is obtained in the same way for the even  $i$  and odd  $i$  cases. By evaluating (3.12) at  $\beta_{i-1}$ , the error is expressed in terms of the error on subdomains of the opposite parity – if  $i$  is even then  $i \pm 1$  is odd, and vice-versa. We use (3.12) twice more to eliminate these terms and we obtain an expression for  $e_i^{n+1}(\beta_{i-1})$  in terms of solution values of subdomains with the same parity at the previous iteration. Taking absolute values, using the triangle inequality and noting  $r_i, p_i, q_i$  and  $s_i$  are non-negative gives the result. Inequality (3.14) is obtained in a similar way.  $\square$

The right hand sides of these bounds are identical to those obtained in the parallel multidomain classical Schwarz method presented in [7], hence convergence follows immediately from the proof of those results, leading to the following theorem.

**THEOREM 3.6.** *Under the assumptions of Lemma 2.1 and the restrictions on the partitioning of  $\Omega_c$  detailed above, the red–black alternating classical Schwarz iteration (3.10 - 3.11) converges globally on an arbitrary number of subdomains.*

If we assume the overlaps are all of the same size, we have the following error estimate.

**THEOREM 3.7.** *The red-black Schwarz iteration (3.10 - 3.11) on  $S$  subdomains with a common overlap ratio  $r \in (0, 0.5]$  converges in the infinity norm and the iterates satisfy*

$$\begin{aligned} \max_{1 \leq 2i \leq S} \|x_{2i}^{n+1}(\xi) - x(\xi)\|_\infty &\leq \left(1 - 4r(1-r) \sin^2 \frac{\pi}{2(S+1)}\right)^n \frac{1}{\tilde{m}} \|e^0\|_2, \\ \max_{1 \leq 2i+1 \leq S} \|x_{2i+1}^{n+1}(\xi) - x(\xi)\|_\infty &\leq \left(1 - 4r(1-r) \sin^2 \frac{\pi}{2(S+1)}\right)^n \frac{1}{\tilde{m}} \|\hat{e}^0\|_2. \end{aligned}$$

If we compare the contraction estimates for the red–black algorithm of Theorem 3.7 to the parallel classical Schwarz algorithm considered in [7], we see that the iteration (3.10 - 3.11) will satisfy the same error bound in  $n$  iterations that the parallel iteration will in  $2n$  iterations. A single iteration of (3.10 - 3.11) requires solving one set of subdomain problems in parallel, followed by a second set of subdomain problems solved in parallel, meaning 2 subdomain solves are required per processor for each iteration. As such, a given processor will handle  $2n$  subdomain problems whether the red-black alternating algorithm or the original parallel algorithm is used. However, the red-black method will only require half the number of processors for each set of parallel computations.

**4. An Alternating Classical Schwarz Method for Time Dependent Mesh Generation.** We now consider the solution of the semi-discretized moving mesh PDE (1.4). We discretize in time via backward Euler and solve the sequence of elliptic problems

$$x^k - \frac{\Delta t}{\tau} (M(x^k) x_\xi^k)_\xi = x^{k-1}, \quad k = 1, 2, \dots,$$

using an alternating classical Schwarz iteration. Here  $k$  is the time step counter.

The parallel classical Schwarz algorithm on two subdomains (only) for this sequence of (nonlinear) elliptic problems was considered in [7]. Here we provide the first extension to an arbitrary number of subdomains for time dependent mesh generation. The analogous result for the parallel algorithm can be adapted from the proof of Theorem 4.2 below.

We decompose  $\Omega = [0, 1]$  into  $S$  subdomains  $\Omega_i = [\alpha_i, \beta_i]$  for  $i = 1, \dots, S$ , where  $\alpha_{i+1} < \beta_i$  for  $i = 1, \dots, S-1$  and  $\beta_i < \alpha_{i+2}$  for  $i = 1, \dots, S-2$ . This leads to the

alternating classical Schwarz iteration for each time step: for  $n = 1, 2, \dots$

$$(4.1) \quad \begin{aligned} x_i^{k,n} - \frac{\Delta t}{\tau} (M(x_i^{k,n}) x_{i,\xi}^{k,n})_\xi &= x^{k-1}, \quad \xi \in \Omega_i \\ x_i^{k,n}(\alpha_i, t_k) &= x_{i-1}^{k,n}(\alpha_i, t_k), \\ x_i^{k,n}(\beta_i, t_k) &= x_{i+1}^{k,n-1}(\beta_i, t_k), \end{aligned}$$

for  $i = 1, \dots, S$ , where  $k$  and  $n$  are time and iteration counters, and  $x_0^{k,n}(\alpha_1, t) \equiv 0$  and  $x_{S+1}^{k,n}(\beta_S, t) \equiv 1$ . The parameter  $\Delta t$  is the user specified time step and  $\tau$  is the mesh relaxation time – for details refer to [14]. For the initial solution  $x^0$  one can simply take a uniformly distributed mesh or a mesh which equidistributes the initial physical solution.

A contraction rate will be obtained by the method of supersolutions and the comparison principle found in [10], which we state in the following Lemma.

LEMMA 4.1. *Suppose  $Lu = au'' + bu' + cu$  is a linear, elliptic operator with  $c \leq 0$  in a bounded domain  $\Omega$ . Suppose that in  $\Omega$ ,  $Lu \geq 0$  ( $\leq 0$ ) with  $u \in C^2(\Omega) \cup C^0(\bar{\Omega})$ . Then*

$$\sup_{\Omega} u \leq \sup_{\partial\Omega} \max(u, 0) \quad \left( \inf_{\Omega} u \geq \inf_{\partial\Omega} \min(u, 0) \right).$$

With this Lemma, we can now prove the following Theorem.

THEOREM 4.2. *Under the assumptions of Lemma 2.1 and the restrictions on the partitioning of  $\Omega_c$  described above, the alternating classical Schwarz iteration (4.1) for the semi-discretized moving mesh PDE (1.4) converges on an arbitrary number of subdomains for any time step  $\Delta t > 0$  and for any mesh relaxation parameter  $\tau > 0$ .*

Furthermore, in the case of two subdomains we have the linear convergence estimates

$$(4.2) \quad \begin{aligned} \|x^k - x_1^{k,n+1}\|_\infty &\leq \rho_{time}^n \frac{\hat{m}}{\check{m}} |x^k(\alpha) - x_1^{k,0}(\alpha)|, \\ \|x^k - x_2^{k,n+1}\|_\infty &\leq \rho_{time}^n \frac{\hat{m}}{\check{m}} |x^k(\beta) - x_2^{k,0}(\beta)|, \end{aligned}$$

where the contraction rate is bounded by

$$(4.3) \quad \rho_{time} = \frac{\sinh(\sqrt{\theta}\alpha) \sinh(\sqrt{\theta}(1-\beta))}{\sinh(\sqrt{\theta}\beta) \sinh(\sqrt{\theta}(1-\alpha))} < 1, \quad \theta = \frac{\tau}{\Delta t} \frac{1}{\hat{m}}.$$

For  $S \geq 3$  subdomains we have the estimates

$$\max_{1 \leq i \leq S} \|x_i^{k,n}(\xi) - x^k(\xi)\|_\infty \leq \rho_{time}^n \frac{1}{\check{m}} \|e^{k,0}\|_2,$$

where the contraction rate is bounded by:

$$\rho_{time} \leq r + \frac{p^2(1-r^{S-2})}{1-r},$$

with  $p$  and  $r$  as defined in (4.9).

*Proof.*

We define error measures

$$(4.4) \quad e_i^{k,n}(\xi) = \int_{x_i^{k,n}(\xi)}^{x^k(\xi)} M d\tilde{x}$$

for  $i = 1, \dots, S$ . Upon differentiation, we see that

$$(4.5) \quad \frac{de_i^{k,n}}{d\xi} = M(x^k) \frac{dx^k}{d\xi} - M(x_i^{k,n}) \frac{dx_i^{k,n}}{d\xi}.$$

From the mean value theorem for integrals we have

$$(4.6) \quad e_i^{k,n} = M(x_i^*)(x^k - x_i^{k,n}),$$

for some  $x_i^*$  between  $x^k$  and  $x_i^{k,n}$ . By subtracting the equation for  $x_i^{k,n}$  from the single domain equation we obtain

$$x^k - x_i^{k,n} - \frac{\Delta t}{\tau} \left( M(x^k) x_\xi^k - M(x_i^{k,n}) x_{i,\xi}^{k,n} \right)_\xi = 0,$$

which, after making the substitutions of (4.5) and (4.6), leads to the iteration, for each  $i = 1, \dots, S$  and for  $n = 1, 2, \dots$

$$\begin{aligned} \frac{d^2 e_i^{k,n}}{d\xi^2} - \frac{\tau}{\Delta t} \frac{1}{M(x_i^*)} e_i^{k,n} &= 0, \quad \xi \in (\alpha_i, \beta_i), \\ e_i^{k,n}(\alpha_i, t_k) &= e_{i-1}^{k,n}(\alpha_i, t_k), \\ e_i^{k,n}(\beta_i, t_k) &= e_{i+1}^{k,n-1}(\beta_i, t_k). \end{aligned}$$

To construct a supersolution for the error on a given subdomain, we let  $\tilde{e}_i^{k,n}$  be the solution of

$$\begin{aligned} \frac{d^2 \tilde{e}_i^{k,n}}{d\xi^2} - \frac{\tau}{\Delta t} \frac{1}{\hat{m}} \tilde{e}_i^{k,n} &= 0, \quad \xi \in (\alpha_i, \beta_i), \\ \tilde{e}_i^{k,n}(\alpha_i) &= |e_{i-1}^{k,n}(\alpha_i)|, \\ \tilde{e}_i^{k,n}(\beta_i) &= |e_{i+1}^{k,n-1}(\beta_i)|, \end{aligned}$$

where, as previously stated,  $\hat{m}$  is the upper bound of  $M$ . We now show  $\tilde{e}_i^{k,n}$  is a supersolution for  $e_i^{k,n}$ . To this end we define

$$d_i^{k,n} = e_i^{k,n} - \tilde{e}_i^{k,n},$$

which satisfies

$$(4.7) \quad \frac{d^2 d_i^{k,n}}{d\xi^2} - \frac{\tau}{\Delta t} \frac{1}{M(x_i^*)} e_i^{k,n} + \frac{\tau}{\Delta t} \frac{1}{\hat{m}} \tilde{e}_i^{k,n} = 0.$$

Adding and subtracting

$$(4.8) \quad \frac{\tau}{\Delta t} \frac{1}{M(x_i^*)} \tilde{e}_i^{k,n}$$

to (4.7) we see the  $d_i^{k,n}$  satisfies

$$\begin{aligned} \frac{d^2 d_i^{k,n}}{d\xi^2} - \frac{\tau}{\Delta t} \frac{1}{M(x_1^*)} d_i^{k,n} &= \frac{\tau}{\Delta t} \left( \frac{1}{M(x_1^*)} - \frac{1}{\hat{m}} \right) \tilde{e}_i^{k,n}, \\ d_i^{k,n}(\alpha_i) &= e_{i-1}^{k,n}(\alpha_i) - |e_{i-1}^{k,n}(\alpha_i)|, \\ d_i^{k,n}(\beta_i) &= e_{i+1}^{k,n-1}(\beta_i) - |e_{i+1}^{k,n-1}(\beta_i)|. \end{aligned}$$

Since  $\hat{m}$  is an upper bound for  $M(x)$ , the right hand side of the differential equation is non-negative. Both boundary values are non-positive and the coefficient of  $\tilde{e}_i^{k,n}$  in the differential equation is negative. Hence, Lemma 4.1 shows  $d_i^{k,n} \leq 0$ , or  $e_i^{k,n} \leq \tilde{e}_i^{k,n}$ , for all  $\xi \in [\alpha_i, \beta_i]$ .

Now, the quantity

$$\tilde{d}_i^{k,n} = e_i^{k,n} + \tilde{e}_i^{k,n}$$

satisfies

$$\frac{d^2 \tilde{d}_i^{k,n}}{d\xi^2} - \frac{\tau}{\Delta t} \frac{1}{M(x_i^*)} e_i^{k,n} - \frac{\tau}{\Delta t} \frac{1}{\hat{m}} \tilde{e}_i^{k,n} = 0,$$

and by adding and subtracting (4.8), we see that  $\tilde{d}_i^{k,n}$  satisfies

$$\begin{aligned} \frac{d^2 \tilde{d}_i^{k,n}}{d\xi^2} - \frac{\tau}{\Delta t} \frac{1}{M(x_i^*)} \tilde{d}_i^{k,n} &= \frac{\tau}{\Delta t} \left( \frac{1}{\hat{m}} - \frac{1}{M(x_i^*)} \right) \tilde{e}_i^{k,n}, \\ \tilde{d}_i^{k,n}(\alpha_i) &= e_{i-1}^{k,n}(\alpha_i) + |e_{i-1}^{k,n}(\alpha_i)|, \\ \tilde{d}_i^{k,n}(\beta_i) &= e_{i+1}^{k,n-1}(\beta_i) + |e_{i+1}^{k,n-1}(\beta_i)|. \end{aligned}$$

The right hand side of the differential equation is non-positive and the boundary conditions are non-negative. Lemma 4.1 guarantees that  $\tilde{d}_i^{k,n}(\xi) \geq 0$ , or  $e_i^{k,n}(\xi) \geq -\tilde{e}_i^{k,n}(\xi)$ , for all  $\xi \in [\alpha_i, \beta_i]$ . Hence, we have shown for  $\xi \in [\alpha_i, \beta_i]$  that  $|e_i^{k,n}(\xi)| \leq |\tilde{e}_i^{k,n}(\xi)|$ , where the function  $\tilde{e}_i^{k,n}$  has the form

$$\tilde{e}_i^{k,n}(\xi) = |e_{i-1}^{k,n}(\alpha_i)| \frac{\sinh(\sqrt{\theta}(\beta_i - \xi))}{\sinh(\sqrt{\theta}(\beta_i - \alpha_i))} + |e_{i+1}^{k,n-1}(\beta_i)| \frac{\sinh(\sqrt{\theta}(\xi - \alpha_i))}{\sinh(\sqrt{\theta}(\beta_i - \alpha_i))},$$

and

$$\theta = \frac{\tau}{\Delta t} \frac{1}{\hat{m}}.$$

We now introduce the following quantities:

$$(4.9) \quad \begin{aligned} r_i &= \frac{\sinh(\sqrt{\theta}(\beta_{i-1} - \alpha_i))}{\sinh(\sqrt{\theta}(\beta_i - \alpha_i))}, & p_i &= \frac{\sinh(\sqrt{\theta}(\beta_i - \beta_{i-1}))}{\sinh(\sqrt{\theta}(\beta_i - \alpha_i))}, \\ q_i &= \frac{\sinh(\sqrt{\theta}(\alpha_{i+1} - \alpha_i))}{\sinh(\sqrt{\theta}(\beta_i - \alpha_i))}, & s_i &= \frac{\sinh(\sqrt{\theta}(\beta_i - \alpha_{i+1}))}{\sinh(\sqrt{\theta}(\beta_i - \alpha_i))}. \end{aligned}$$

Once again if we have equal sized subdomains and a common overlap ratio we introduce the quantities  $r, s, p$  and  $q$ , where  $r = s$ , and  $p = q$ .

By analysis similar to that of the steady case (see the proof of Lemma 3.2), we find that the error at the interface  $\xi = \beta_{i-1}$ ,  $i = 2, \dots, S$  satisfies

$$|e_i^{k,n}(\beta_{i-1})| \leq p_i \sum_{j=2}^i \left( q_{j-1} \prod_{\ell=j}^{i-1} s_\ell |e_j^{k,n-1}(\beta_{j-1})| \right) + r_i |e_{i+1}^{k,n-1}(\beta_i)|,$$

while at  $\xi = \alpha_{i+1}$ ,  $i = 1, \dots, S-1$  we have

$$|e_i^{k,n}(\alpha_{i+1})| \leq \sum_{j=2}^{i+1} \left( q_{j-1} \prod_{\ell=j}^i s_\ell |e_j^{k,n-1}(\beta_{j-1})| \right),$$

where we define  $\prod_{\ell=i}^{i-1} s_\ell = 1$ . As in the steady case, we can restrict our attention to the  $\beta$  interfaces. Writing these inequalities in matrix form, we find

$$(4.10) \quad \mathbf{e}^{k,n+1} \leq M_e \mathbf{e}^{k,n},$$

where

$$\mathbf{e}^{k,n} = (|e_2^{k,n}(\beta_1)|, |e_3^{k,n}(\beta_2)|, \dots, |e_S^{k,n}(\beta_{S-1})|)^T$$

and the  $(S-1) \times (S-1)$  matrix is given as

$$M_e = \begin{bmatrix} p_2 q_1 & r_2 & & & & & & & & \\ p_3 s_2 q_1 & p_3 q_2 & r_3 & & & & & & & \\ p_4 s_3 s_2 q_1 & p_4 s_3 q_2 & p_4 q_3 & r_4 & & & & & & \\ \vdots & \vdots & \vdots & \ddots & \ddots & & & & & \\ & & & & & p_{S-1} q_{S-2} & r_{S-1} & & & \\ p_S s_{S-1} \cdots s_2 q_1 & \cdots & & & & p_S s_{S-1} q_{S-2} & p_S q_{S-1} & & & \end{bmatrix}.$$

To demonstrate convergence, we wish to show that  $\rho(M_e) < 1$ . First, we show that the quantities (4.9) are strictly less than the steady quantities (3.5). Differentiating the function

$$f(x) = \frac{\sinh(x)}{x},$$

it is easy to see  $f$  is increasing for all  $x > 0$ . Thus, for  $0 < a < b$  we have

$$\frac{\sinh(a)}{a} < \frac{\sinh(b)}{b} \quad \text{or} \quad \frac{\sinh(a)}{\sinh(b)} < \frac{a}{b}.$$

It now follows from the steady case analysis that  $\|M_e\|_\infty < 1$ , as all row sums will be smaller in magnitude than their steady counterparts, and hence we have convergence.

For the two subdomain iteration,

$$\begin{aligned} x_1^{k,n} - \frac{\Delta t}{\tau} (M(x_1^{k,n}) x_{1,\xi}^{k,n})_\xi &= x^{k-1}, & x_2^{k,n} - \frac{\Delta t}{\tau} (M(x_2^{k,n}) x_{2,\xi}^{k,n})_\xi &= x^{k-1}, \\ x_1^{k,n}(0, t_k) &= 0, & x_2^{k,n}(\alpha, t_k) &= x_1^{k,n}(\alpha, t_k), \\ x_1^{k,n}(\beta, t_k) &= x_2^{k,n-1}(\beta, t_k), & x_2^{k,n}(1, t_k) &= 1. \end{aligned}$$

the matrix  $M_e$  is reduced to the single scalar value  $p_2 q_1$ , which is our contraction rate,  $\rho_{\text{time}}$ . Substituting the expressions for  $p_2$  and  $q_1$ , we find

$$\rho_{\text{time}} = \frac{\sinh(\sqrt{\theta}\alpha) \sinh(\sqrt{\theta}(1-\beta))}{\sinh(\sqrt{\theta}\beta) \sinh(\sqrt{\theta}(1-\alpha))} < 1, \quad \theta = \frac{\tau}{\Delta t} \frac{1}{\hat{m}},$$

which is the same contraction rate obtained in the parallel two subdomain case of [7].

For  $S \geq 3$  subdomains, if we make the simplifying assumption that all subdomains are of equal size and each pair of adjacent subdomains have equal amounts of overlap, then we have the iteration matrix

$$M_e = \begin{bmatrix} p^2 & r & & & & & & & & \\ p^2 r & p^2 & r & & & & & & & \\ p^2 r^2 & p^2 r & p^2 & r & & & & & & \\ \vdots & \vdots & \vdots & \ddots & \ddots & & & & & \\ & & & & & p^2 & r & & & \\ p^2 r^{S-2} & \cdots & & & & p^2 r & p^2 & & & \end{bmatrix}.$$







Substituting these last three relations into the transmission conditions (5.2) and (5.3) and rearranging, we obtain

$$(5.8) \quad \alpha_i z_i^{+,n} - \beta_i z_i^{-,n} = \frac{\beta_i - \alpha_i}{\beta_{i-1} - \alpha_{i-1}} [\alpha_{i-1} z_{i-1}^{+,n} - \beta_{i-1} z_{i-1}^{-,n}],$$

for  $i = 2, \dots, S$ , and

$$(5.9) \quad (1 - \alpha_i) z_i^{+,n} - (1 - \beta_i) z_i^{-,n} = \frac{\beta_i - \alpha_i}{\beta_{i+1} - \alpha_{i+1}} [(1 - \alpha_{i+1}) z_{i+1}^{+,n-1} - (1 - \beta_{i+1}) z_{i+1}^{-,n-1}],$$

for  $i = 1, \dots, S-1$ .

Multiplying (5.8) by  $(1 - \alpha_i)$  and (5.9) by  $\alpha_i$ , and taking the difference gives

$$(5.10) \quad \begin{aligned} z_i^{-,n} &= \frac{1 - \alpha_i}{\beta_{i-1} - \alpha_{i-1}} [\beta_{i-1} z_{i-1}^{-,n} - \alpha_{i-1} z_{i-1}^{+,n}] \\ &\quad - \frac{\alpha_i}{\beta_{i+1} - \alpha_{i+1}} [(1 - \beta_{i+1}) z_{i+1}^{-,n-1} - (1 - \alpha_{i+1}) z_{i+1}^{+,n-1}]. \end{aligned}$$

Similarly, multiplying (5.8) by  $(1 - \alpha_i)(\alpha_{i+1} - \alpha_i)$  and (5.9) by  $\alpha_i(\alpha_{i-1} - \alpha_{i-2})$ , and taking the difference we have

$$(5.11) \quad \begin{aligned} z_i^{+,n} &= \frac{1 - \beta_i}{\beta_{i-1} - \alpha_{i-1}} [\beta_{i-1} z_{i-1}^{-,n} - \alpha_{i-1} z_{i-1}^{+,n}] \\ &\quad - \frac{\beta_i}{\beta_{i+1} - \alpha_{i+1}} [(1 - \beta_{i+1}) z_{i+1}^{-,n-1} - (1 - \alpha_{i+1}) z_{i+1}^{+,n-1}]. \end{aligned}$$

The expressions (5.10) and (5.11) hold for  $i = 3, \dots, S-2$ . The cases  $i = 1, 2, S-1$ , and  $i = S$  are somewhat different, they are given by:

$$(5.12) \quad \begin{aligned} z_1^{-,n} &= 0, \\ z_1^{+,n} &= -\frac{\beta_1}{\beta_2 - \alpha_2} [(1 - \beta_2) z_2^{-,n-1} - (1 - \alpha_2) z_2^{+,n-1}], \\ z_2^{-,n} &= -\frac{\alpha_2}{\beta_3 - \alpha_3} [(1 - \beta_3) z_3^{-,n-1} - (1 - \alpha_3) z_3^{+,n-1}] \\ z_2^{+,n} &= -\frac{\beta_2}{\beta_3 - \alpha_3} [(1 - \beta_3) z_3^{-,n-1} - (1 - \alpha_3) z_3^{+,n-1}], \\ z_{S-1}^{-,n} &= \frac{1 - \alpha_{S-1}}{\beta_{S-2} - \alpha_{S-2}} [\beta_{S-2} z_{S-2}^{-,n} - \alpha_{S-2} z_{S-2}^{+,n}] + \alpha_{S-1} C, \\ z_{S-1}^{+,n} &= \frac{1 - \beta_{S-1}}{\beta_{S-2} - \alpha_{S-2}} [\beta_{S-2} z_{S-2}^{-,n} - \alpha_{S-2} z_{S-2}^{+,n}] + \beta_{S-1} C, \\ z_S^{-,n} &= \frac{1 - \alpha_S}{\beta_{S-1} - \alpha_{S-1}} [\beta_{S-1} z_{S-1}^{-,n} - \alpha_{S-1} z_{S-1}^{+,n}] + \alpha_S C, \\ z_S^{+,n} &= C, \end{aligned}$$

where

$$C = \int_0^1 M(\tilde{x}) d\tilde{x}.$$

A straightforward check shows that the difference equations (5.10–5.12) can be expressed as a matrix iteration

$$Az^n = Bz^{n-1} + c,$$

where  $z$  is defined in (5.4),  $A$  and  $B$  are given in (5.5) and (5.6), and  $c$  is a vector which does not depend on the iteration number.  $\square$

To establish convergence of the iteration  $Az^n = Bz^{n-1} + c$ , we have to analyze the matrix  $A^{-1}B$ . We begin with the following Lemma which characterizes the matrix  $A^{-1}$ .

LEMMA 5.2. *The matrix  $C = A^{-1}$  is block lower triangular matrix with blocks*

$$(5.13) \quad C^{i,j} = \begin{cases} 0_{2 \times 2} & \text{if } j > i, \\ I_{2 \times 2} & \text{if } j = i, \\ 0_{2 \times 2} & \text{if } j < i, j = 1, \\ (-1)^{i+j} L_i L_{i+1} \cdots L_{j+1} & \text{if } j < i, j > 1. \end{cases}$$

*Proof.* Since  $A$  has a nonzero determinant it is invertible. The inverse of  $A$  may be computed recursively using the block inverse formula

$$\begin{pmatrix} I & 0 \\ R & S \end{pmatrix}^{-1} = \begin{pmatrix} I & 0 \\ -S^{-1}R & S^{-1} \end{pmatrix}.$$

Here the column dimension of  $I$  and  $R$ , the row dimension of  $R$  and  $S$ , the column dimension of  $O$  and  $S$ , and the row dimension of  $I$  and  $O$  are assumed to be the same. Of course  $S$  is assumed to be nonsingular.

As example we can compute

$$\begin{pmatrix} I_{2 \times 2} & 0_{2 \times 2} \\ L_S & I_{2 \times 2} \end{pmatrix}^{-1} = \begin{pmatrix} I_{2 \times 2} & 0_{2 \times 2} \\ -L_S & I_{2 \times 2} \end{pmatrix}$$

and then use the block inverse formula to compute

$$\begin{pmatrix} I_{2 \times 2} & 0_{2 \times 2} & 0_{2 \times 2} \\ L_{S-1} & I_{2 \times 2} & 0_{2 \times 2} \\ 0_{2 \times 2} & L_S & I_{2 \times 2} \end{pmatrix}^{-1} = \begin{pmatrix} I_{2 \times 2} & 0_{2 \times 2} & 0_{2 \times 2} \\ -L_{S-1} & I_{2 \times 2} & 0_{2 \times 2} \\ L_S L_{S-1} & -L_S & I_{2 \times 2} \end{pmatrix}.$$

Continuing in this fashion, we can explicitly compute the blocks of  $A^{-1}$  as specified in (5.13). Of course one can explicitly check the validity of (5.13) by multiplication by the matrix  $A$  to recover the identity.  $\square$

The following Lemma is useful to understand the iteration matrix  $A^{-1}B$  and follows by direct calculation.

LEMMA 5.3. *For  $i = 2, \dots, S-2$ , we have  $U_i L_{i+1} = 0_{2 \times 2} = L_{i+1} U_i$ .*

We now arrive at the main result of this section.

THEOREM 5.4. *The alternating Schwarz iteration (5.1)–(5.3) is optimal on  $S$  subdomains; convergence is obtained in  $S$  iterations.*

*Proof.* Writing  $A^{-1}$  as  $\text{tril}(C) + I$ , where  $\text{tril}(C)$  denotes the strictly lower triangular part of  $C$ , we have  $A^{-1}B = \text{tril}(C)B + B$ . Using Lemma 5.3 and computing directly we find  $\text{tril}(C)B = 0$  and hence  $A^{-1}B$  is the strictly upper triangular matrix  $B$ . A well known property of strictly triangular matrices is that they are nilpotent; in this case  $B^S = 0$ . Since the error after  $S$  iterations is  $e^S = B^S e^0$  then we have finite convergence after  $S$  iterations.  $\square$

The optimal transmission conditions can be applied on non-overlapping subdomains as well without affecting the convergence. The analysis is a simple modification of that presented above by simplifying choosing  $\alpha_{i+1} = \beta_i$ , cf. Figure 1.2. Refer to [13] for details.

**6. Alternating Optimized Schwarz.** It was shown in [7] that an optimized Schwarz method can be derived with local nonlinear Robin transmission conditions which approximate the optimal Schwarz transmission conditions discussed in Section 5. The motivation for

doing so is to keep the improved rate of convergence compared to classical Schwarz, while eliminating the need to evaluate the nonlocal integral boundary conditions required in the iteration (5.1)–(5.3).

For completeness, and to facilitate the numerical comparisons we present in Section 7, we quote the analogous alternating optimized Schwarz method for mesh generation in this section. The proof, which is a minor alteration of the result in [7], may be found in [13].

We decompose  $\Omega = [0, 1]$  into two non-overlapping subdomains,  $\Omega_1 = [0, \alpha]$  and  $\Omega_2 = [\alpha, 1]$ . The alternating optimized Schwarz iteration to solve (1.3) is

$$(6.1) \quad \begin{aligned} (M(x_1^n)x_{1,\xi}^n)_\xi = 0, \quad \xi \in \Omega_1, & & (M(x_2^n)x_{2,\xi}^n)_\xi = 0, \quad \xi \in \Omega_2, \\ x_1^n(0) = 0, & & \tilde{\mathcal{B}}_2(x_2^n(\alpha)) = \tilde{\mathcal{B}}_2(x_1^n(\alpha)), \\ \tilde{\mathcal{B}}_1(x_1^n(\alpha)) = \tilde{\mathcal{B}}_1(x_2^{n-1}(\alpha)) & & x_2^n(1) = 1, \end{aligned}$$

where the nonlinear transmission operators  $\tilde{\mathcal{B}}_i$ ,  $i = 1, 2$  are given by

$$(6.2) \quad \tilde{\mathcal{B}}_1(\cdot) \equiv M(\cdot)\partial_\xi(\cdot) + pI(\cdot), \quad \text{and} \quad \tilde{\mathcal{B}}_2(\cdot) \equiv M(\cdot)\partial_\xi(\cdot) - pI(\cdot).$$

As shown in [7],  $\tilde{\mathcal{B}}_{1,2}$  can be seen as approximations to  $\mathcal{B}_{1,2}$ .

To simplify the presentation, we introduce the operators  $R_1$  and  $R_2$ , where

$$(6.3) \quad R_1(x) = \frac{1}{\alpha} \int_0^x M(\tilde{x}) d\tilde{x} \quad \text{and} \quad R_2(x) = \frac{1}{1-\alpha} \int_x^1 M(\tilde{x}) d\tilde{x},$$

and use them to express both the implicit subdomain solutions and the optimized iteration, as described in Lemma 6.1.

LEMMA 6.1. *Under the assumptions of Lemmas 2.4 and 2.5, the subdomain solutions on  $\Omega_1$  and  $\Omega_2$  of (6.1) are given implicitly by the formulas*

$$\int_0^{x_1^n(\xi)} M(\tilde{x}) d\tilde{x} = R_1(x_1^n(\alpha))\xi \quad \text{and} \quad \int_{x_2^n(\xi)}^1 M(\tilde{x}) d\tilde{x} = R_2(x_2^n(\alpha))(1-\xi).$$

Furthermore, the Robin conditions at the interface force the operator values to satisfy the recurrence relations:

$$(6.4) \quad R_1(x_1^{n+1}(\alpha)) + px_1^{n+1}(\alpha) = R_2(x_2^n(\alpha)) + px_2^n(\alpha)$$

and

$$(6.5) \quad R_2(x_2^n(\alpha)) - px_2^n(\alpha) = R_1(x_1^n(\alpha)) - px_1^n(\alpha).$$

This representation of the iteration allows us to prove the following result, again see [13] for the details of the proof.

THEOREM 6.2. *Under the assumptions of Lemma 2.1 the iteration (6.4–6.5) converges globally to the exact solution  $x(\alpha)$  for all  $p > 0$ . Moreover, we have the linear convergence estimate*

$$\begin{aligned} \|x - x_1^n\|_\infty &\leq \frac{\hat{m}}{\check{m}} \cdot \frac{p + \frac{1}{\alpha}\hat{m}}{p + \frac{1}{\alpha}\check{m}} \rho_{\text{robin}}^n |x(\alpha) - x_1^0(\alpha)|, \\ \|x - x_2^n\|_\infty &\leq \frac{\hat{m}}{\check{m}} \cdot \frac{p + \frac{1}{1-\alpha}\hat{m}}{p + \frac{1}{1-\alpha}\check{m}} \rho_{\text{robin}}^n |x(\alpha) - x_2^0(\alpha)|, \end{aligned}$$

where an estimate on the contraction factor is

$$(6.6) \quad \rho_{robin} = \sqrt{\frac{p^2 + \frac{\hat{m}^2}{(1-\alpha)^2} - 2p\frac{\hat{m}}{1-\alpha}}{p^2 + \frac{\hat{m}^2}{(1-\alpha)^2} + 2p\frac{\hat{m}}{1-\alpha}}} \cdot \sqrt{\frac{p^2 + \frac{\hat{m}^2}{\alpha^2} - 2p\frac{\hat{m}}{\alpha}}{p^2 + \frac{\hat{m}^2}{\alpha^2} + 2p\frac{\hat{m}}{\alpha}}}.$$

The expression (6.6) allows one to *optimize* the choice of  $p$  to minimize the contraction rate.

**7. Numerical Results.** When computing the desired mesh transformation, the function  $u(x)$  or  $u(x, t)$  is often not known a priori – instead it is the solution of the physical PDE of interest. As such, the physical solution and mesh transformation are coupled. In practice, however, the physical PDE and mesh PDE are solved in an iterative fashion. This justifies the analysis presented in this paper which focuses solely on the generation of the mesh assuming  $u(x)$  or  $u(x, t)$  is known.

The choice of mesh density function is often application dependent [15]. In the following examples, we simply choose the arc-length mesh density function

$$M(x) = \sqrt{1 + \left(\frac{du}{dx}\right)^2},$$

due to the ease of implementation and interpretation. This mesh density function will force mesh points to regions of rapid change in the  $u$  values. For a particular time independent choice of  $u(x)$ , we use the function

$$u(x) = \frac{1 - \exp(20x)}{1 - \exp(20)},$$

which exhibits a boundary layer at  $x = 1$ , requiring a locally fine mesh to resolve the function adequately.

In Figure 7.1 we present convergence histories which report the maximum observed error, in the infinity norm, between the single domain mesh  $x(\xi)$  and the DD solutions  $x_{1,2}^n(\xi)$ . On the left we present the alternating classical Schwarz algorithm of Section 3.1 and on the right the red-black alternating version of Section 3.2. We use 4 subdomains, with a minimum of 100 mesh points; the exact number varying slightly to ensure that each subdomain is of equal size. As recorded in the figure, by increasing the amount of overlap and hence the number of mesh points shared by adjacent subdomains, we can significantly improve the rate of convergence of the DD algorithm. The unfortunate trade-off is that by increasing the amount of overlap we make each subdomain larger, hence each subdomain solve becomes more costly in terms of computation time. Perhaps the more interesting observation is the similarity between the plots on the left and the right. The rate of convergence is essentially unaffected by the choice of algorithm, suggesting that the red-black algorithm can enjoy both the rate of convergence of an alternating method while still taking advantage of a parallel implementation.

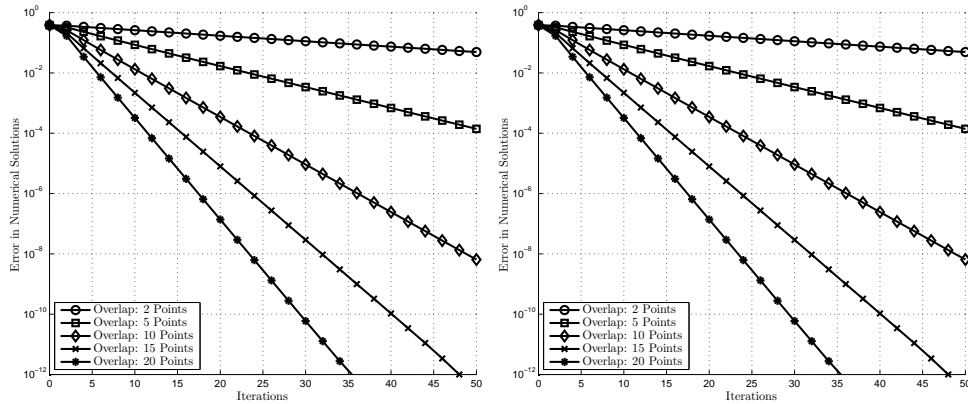


FIG. 7.1. Classical Schwarz convergence histories for the alternating method (left) and the red-black alternating method (right) for varying amounts of subdomain overlap measured by number of common mesh points.

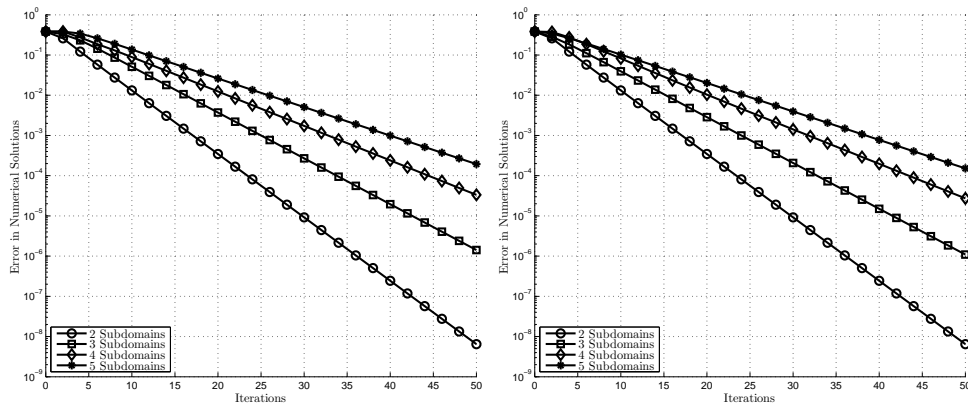


FIG. 7.2. Classical Schwarz convergence histories for alternating (left) and red-black coloring alternating (right) methods illustrating the effect increasing the number of subdomains on the rate of convergence.

In Figure 7.2 we again consider the alternating and red-black Schwarz methods (left and right, respectively), now indicating how the rate of convergence varies with the number of subdomains used. We use a minimum of 100 mesh points throughout the entire domain, and require an overlap of 10 mesh points between each pair of adjacent subdomains. For both methods, the general trend is that as the number of subdomains increase, the rate of convergence experiences a corresponding decrease. This is expected, for when there are  $S$  subdomains, changes in the leftmost subdomain solution will only effect the rightmost subdomain solution after  $S$  DD iterations, and vice versa. This degradation of the convergence rate can be dealt with by a coarse correction [16].

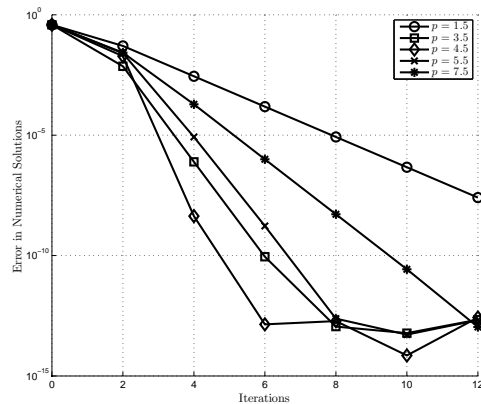


FIG. 7.3. Convergence histories for the alternating optimized Schwarz algorithm illustrating the effect of the parameter  $p$  on the rate of convergence.

In Figure 7.3 we illustrate how the parameter  $p$  in the optimized transmission condition (6.2) affects the rate of convergence of the non-overlapping alternating optimized Schwarz method presented in Section 6. We consider the case of two non-overlapping subdomains sharing a single mesh point, using a total of 101 mesh points in the entire domain. Increasing the value of  $p$  from 1.5 to 7.5, we observe improved convergence until  $p = 4.5$ , at which point subsequent  $p$  values give poorer results. In general we expect an optimal  $p$  value to exist. If we take  $p$  arbitrarily large, we return to the classical Schwarz case, which will typically fail to give the correct solution without overlap.

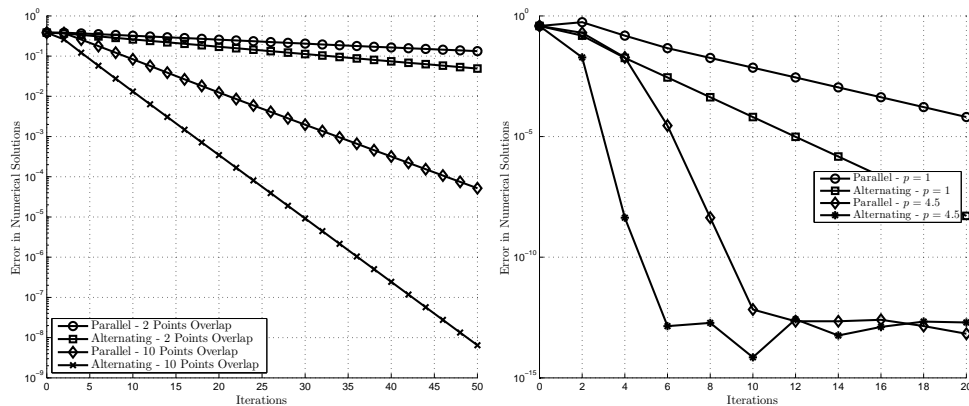


FIG. 7.4. Left: convergence histories comparing the rate of convergence for parallel and alternating classical Schwarz methods with different amounts of overlap. Right: convergence histories comparing parallel and alternating optimized Schwarz for different  $p$  values.

We compare the convergence of alternating and parallel Schwarz iterations, from [7], in Figure 7.4. On the left we compare convergence histories for two different amounts of overlap. In both cases we see that the alternating method outperforms the parallel version in terms of required iteration count to reach a prescribed tolerance. On the right of Figure 7.4 we compare the parallel and alternating optimized Schwarz methods for mesh generation with two different  $p$  values. Again we see that the alternating method converges significantly faster in terms of the number of required iterations.

On the left of Figure 7.5 we compare the alternating and parallel versions of the optimal Schwarz algorithm presented in Section 5 with two different amounts of overlap. Unlike the classical Schwarz method, the increase in overlap only has a small impact on the rate of convergence of the optimal Schwarz algorithm — and only when we discretize and approximate the optimal transmission conditions. Numerically we do not see optimal convergence in two iterations on two subdomains; this is due to the approximation of the transmission conditions via numerical quadrature. In the right hand side plot of Figure 7.5 we show convergence histories for classical, optimized, and optimal Schwarz methods. We use two subdomains with only a shared boundary for optimized and optimal Schwarz, and 10 points of overlap for classical Schwarz. We use  $p = 4.5$  for the optimized parameter, which previously gave the best results. Optimal Schwarz converges fastest, followed by optimized Schwarz, with classical Schwarz a distant third, despite the increased amount of overlap.

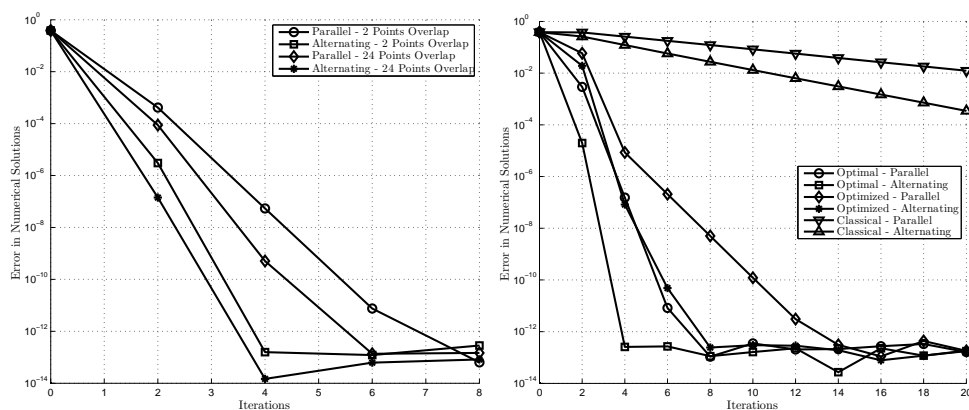


FIG. 7.5. Left: convergence histories comparing the rate of convergence of parallel and alternating optimal Schwarz methods for different amounts of subdomain overlap. Right: convergence histories offering a general comparison of parallel and alternating versions of the classical, optimized, and optimal Schwarz iterations.

The purpose of these algorithms is to generate meshes to resolve the physical solution  $u(x)$  as well as possible. This provides an alternate means of comparing the algorithms. One possibility is to report the maximum difference between the function  $u(x)$  and the piecewise linear interpolant obtained by using exact values of  $u$  at the mesh points obtained from a given algorithm. We refer to this as the interpolation error for a particular mesh. The interpolation errors, computed using a very fine uniform grid, provide a mesh quality measure for each iteration.

TABLE 7.1  
Interpolation errors for the grids obtained by various alternating Schwarz iterations.

Iterations	0	2	4	6	8	10	$\infty$
Classical	0.3658	0.0468	0.0417	0.0393	0.0381	0.0375	0.0370
Optimized	0.3625	0.0366	0.0366	0.0366	0.0366	0.0366	0.0366
Optimal	0.3625	0.0367	0.0366	0.0366	0.0366	0.0366	0.0366

In Table 7.1 we record the maximum interpolation errors for  $u(x)$  over a given mesh for every second iteration up to and including the tenth. The 0 column records the interpolation error of the initial uniform mesh and the  $\infty$  column records the error over the single domain mesh obtained by solving (1.3). For classical Schwarz we use 100 mesh points over two subdomains with 10 points of overlap, and for the other DD algorithms we use 101 mesh

points over two subdomains with 1 point of overlap and we choose  $p = 4.5$  as the optimized Schwarz parameter. We see that after two iterations the optimized and optimal meshes have the same interpolation error as the single domain mesh. While the classical Schwarz algorithm fails to reach this level of mesh quality after 10 iterations, they still attain a maximum error of  $10^{-2}$  after 2 iterations. As such, while agreement with the single domain mesh may suffer, the meshes obtained with all the DD methods may give a sufficient resolution of  $u(x)$  before convergence.

As a final example, we illustrate the classical Schwarz algorithm for time dependent mesh generation. Here we compute time dependent meshes to equidistribute the arc-length mesh density function for

$$u(x, t) = \frac{1}{2}[1 - \tanh(c(t)(x - t - 0.4))], \quad c(t) = 1 + \frac{199}{2}(1 + \tanh(50(t - 0.05))).$$

In the left of Figure 7.6 we show the convergence of the DD algorithms used to compute the mesh at  $t = 0.1$  using different choices of time steps. We use 50 mesh points over two subdomains with 10 points of overlap and time steps of 0.001, 0.0005 and 0.00025. Unsurprisingly, the general trend observed is that the error at a given iteration is lower for a smaller time step, and the DD iterations for a smaller time step have a better contraction rate. This is consistent with the conclusions of Theorem 4.2. On the right we plot the mesh trajectories of  $x(\xi, t)$ , where each line represents the motion of a single mesh point as time increases. We observe a clustering of mesh points near the middle as a steep front forms and propagates from left to right as time increases.

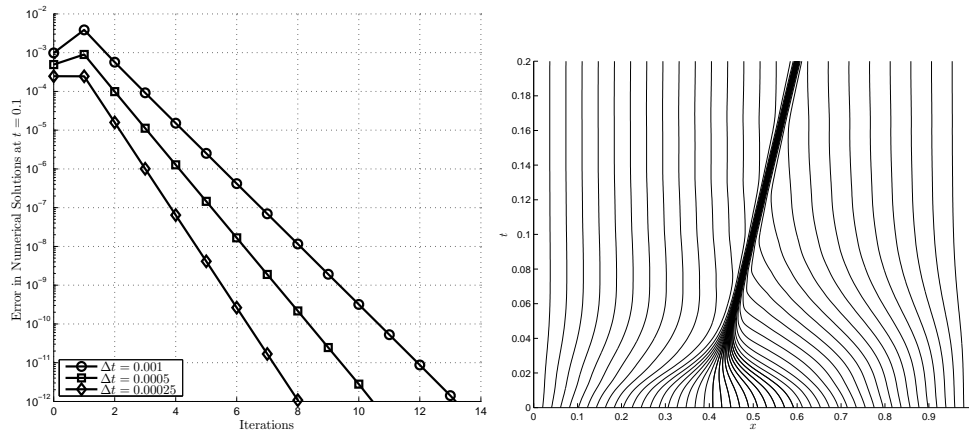


FIG. 7.6. Left: Convergence histories for the time dependent alternating Schwarz iteration for varying choices of  $\Delta t$ . Right: Mesh Trajectory for the function  $x(\xi, t)$ .

**8. Summary.** This paper proposes and analyzes alternating Schwarz methods for solving the nonlinear boundary value problem (1.3), which forms the basis of one dimensional mesh generation by the equidistribution principle. Classical, optimized, and optimal Schwarz iterations have been discussed, with convergence results for a sequential and a red-black Schwarz iteration established. First convergence proofs for the optimal Schwarz method for steady mesh generation and classical Schwarz for time dependent mesh generation on an arbitrary number of subdomains have been provided. The numerical results presented agree with the theory showing that alternating iterations can offer significant improvement in convergence over their parallel counterparts; with the loss of immediate parallelization. However,



as seen in both theoretical and numerical results sections, it is possible to use the red-black method to reap both benefits: experiencing faster convergence than purely parallel iterations but with the option of parallel implementation.

Work is ongoing to develop and analyze DD algorithms for two-dimensional mesh generation, see [11], and coupling the DD algorithms for mesh generation with the DD methods for the physical PDE.

**Acknowledgements** This work was supported (in part) by the Natural Sciences and Engineering Research Council of Canada (NSERC) discovery grant and graduate scholarships programs. The authors would also like to thank Felix Kwok (Geneva) for discussions about this work.

#### REFERENCES

- [1] LUIGI BROCHARD, *Efficiency of multicolor domain decomposition on distributed memory systems*. Domain decomposition methods, Proc. 2nd Int. Symp., Los Angeles/Calif. 1988, 249-259 (1989), 1989.
- [2] CHRIS J. BUDD, WEIZHANG HUANG, AND ROBERT D. RUSSELL, *Adaptivity with moving grids*, Acta Numerica, 18 (2009), pp. 111–241.
- [3] CARL DE BOOR, *Good approximation by splines with variable knots*, in Spline functions and approximation theory (Proc. Sympos., Univ. Alberta, Edmonton, Alta., 1972), Birkhäuser, Basel, 1973, pp. 57–72. Internat. Ser. Numer. Math., Vol. 21.
- [4] ———, *Good approximation by splines with variable knots. ii*, in Conference on the Numerical Solution of Differential Equations, G. Watson, ed., vol. 363 of Lecture Notes in Mathematics, Springer Berlin / Heidelberg, 1974, pp. 12–20. 10.1007/BFb0069121.
- [5] JAMES W. DEMMEL, *Applied Numerical Linear Algebra*, Society for Industrial and Applied Mathematics, Philadelphia, PA, USA, 1997.
- [6] MARTIN J. GANDER, *Schwarz methods over the course of time*, Electron. Trans. Numer. Anal., 31 (2008), pp. 228–255.
- [7] MARTIN J. GANDER AND RONALD D. HAYNES, *Domain decomposition approaches for mesh generation via the equidistribution principle*, SIAM Journal on Numerical Analysis, 50 (2012), pp. 2111–2135.
- [8] MARTIN J. GANDER, RONALD D. HAYNES, AND ALEXANDER J.M. HOWSE, *Alternating and linearized alternating schwarz methods for equidistributing grids*, in Domain Decomposition Methods in Science and Engineering XX, vol. 91 of Lect. Notes Comput. Sci. Eng., Springer-Verlag, 2013, pp. 395–402.
- [9] M. J. GANDER AND A. M. STUART, *Space–time continuous analysis of waveform relaxation for the heat equation*, SIAM J. Sci. Comput., 19 (1998), pp. 2014–2031.
- [10] DAVID GILBARG AND NEIL S. TRUDINGER, *Elliptic Partial Differential Equations of Second Order*, Classics in Mathematics, Springer-Verlag, Berlin, 2001. Reprint of the 1998 edition.
- [11] RONALD D. HAYNES AND ALEXANDER J.M. HOWSE, *Generating equidistributed meshes in 2d via domain decomposition*, in Domain decomposition methods in science and engineering XXI, Lect. Notes Comput. Sci. Eng. In Press.
- [12] RONALD D. HAYNES AND ROBERT D. RUSSELL, *A schwarz waveform moving mesh method*, SIAM Journal on Scientific Computing, 29 (2007), pp. 656–673.
- [13] ALEXANDER J. M. HOWSE, *Domain decomposition approaches for the generation of equidistributing grids*, master’s thesis, Memorial University of Newfoundland, 2013.
- [14] WEIZHANG HUANG, YUHE REN, AND ROBERT D. RUSSELL, *Moving mesh partial differential equations (mmpdes) based on the equidistribution principle*, SIAM Journal on Numerical Analysis, 31 (1994), pp. 709–730.
- [15] WEIZHANG HUANG AND ROBERT D. RUSSELL, *Adaptive Moving Mesh Methods (Applied Mathematical Sciences)*, Springer, 1st edition. ed., Oct. 2010.
- [16] ANDREA TOSELLI AND OLOF B. WIDLUND, *Domain Decomposition Methods – Algorithms and Theory*, Springer series in computational mathematics, 34, Springer, 1 ed., Nov. 2005.
- [17] X. XU, W. HUANG, R. D. RUSSELL, AND J. F. WILLIAMS, *Convergence of de boor’s algorithm for the generation of equidistributing meshes*, IMA Journal of Numerical Analysis, 31 (2011), pp. 580–596.